SUPPLEMENTAL MATERIAL

SUPPLEMENTARY FIGURE LEGENDS

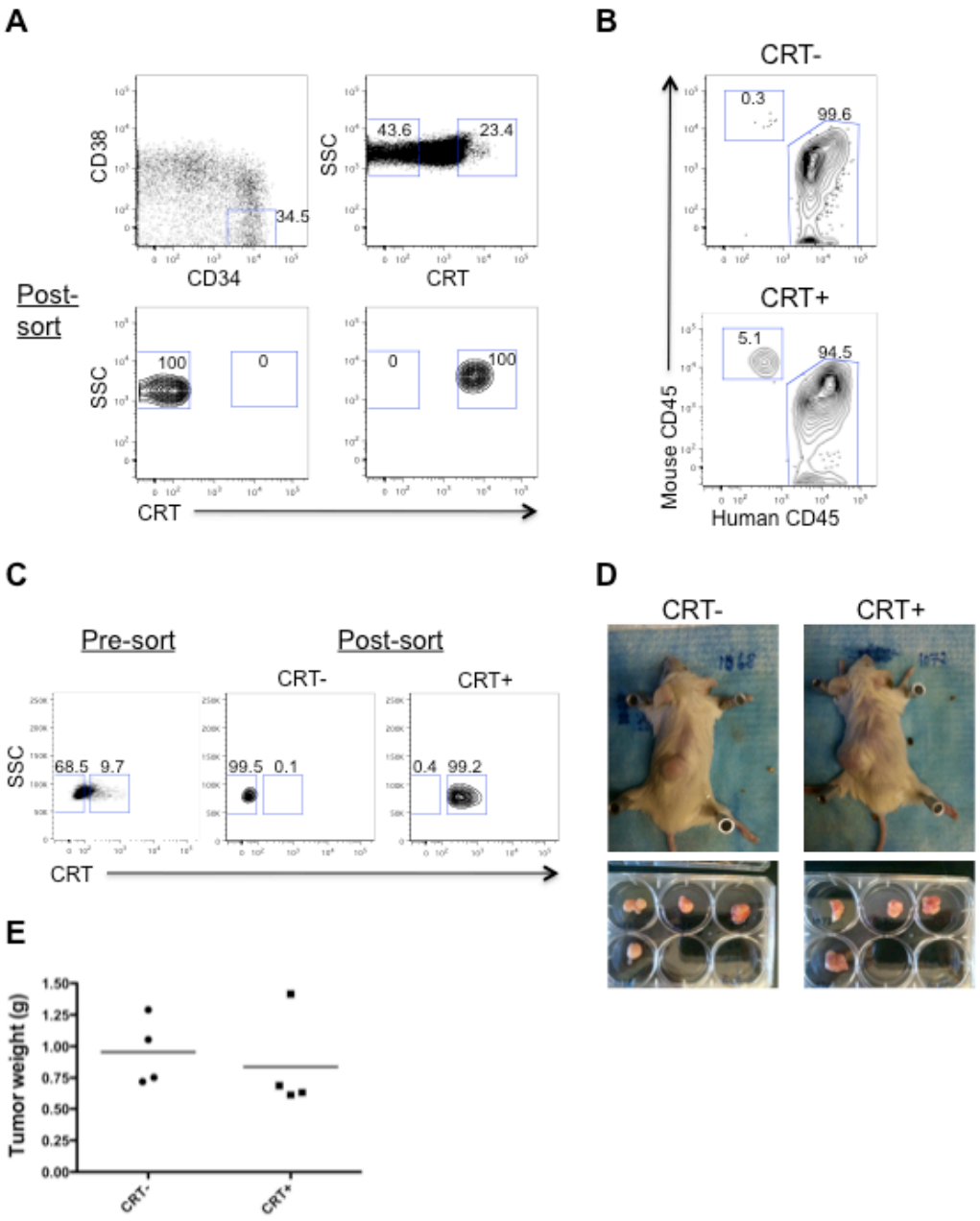

Fig. S1: Live calreticulin positive cancer cells form tumors in vivo
(A) CRT- and CRT+ LSC from human AML patient samples were sorted to 100% purity by FACS. (B) 5,000 CRT- or CRT+ AML LSC were transplanted into the facial vein of sublethally-irradiated newborn NSG. Eight weeks later mice were sacrificed and analyzed for AML bone marrow engraftment. Equal AML engraftment (as shown by human CD45+ chimerism) was observed in both CRT- and CRT+ AML LSC. Representative data are shown. (C) CRT- and CRT+ primary human bladder cancer cells from mouse xenografts were sorted by FACS to >99% purity. (D,E) 10,000 CRT- or CRT+ bladder cancer cells were transplanted subcutaneously onto the flanks of NSG mice. Eight weeks later solid tumor growth was equal in mice transplanted with CRT- and CRT+ cells (D, top panels). CRT+ and CRT-tumors were excised (D, bottom panels), with no difference in tumor weight (E, p=0.63).

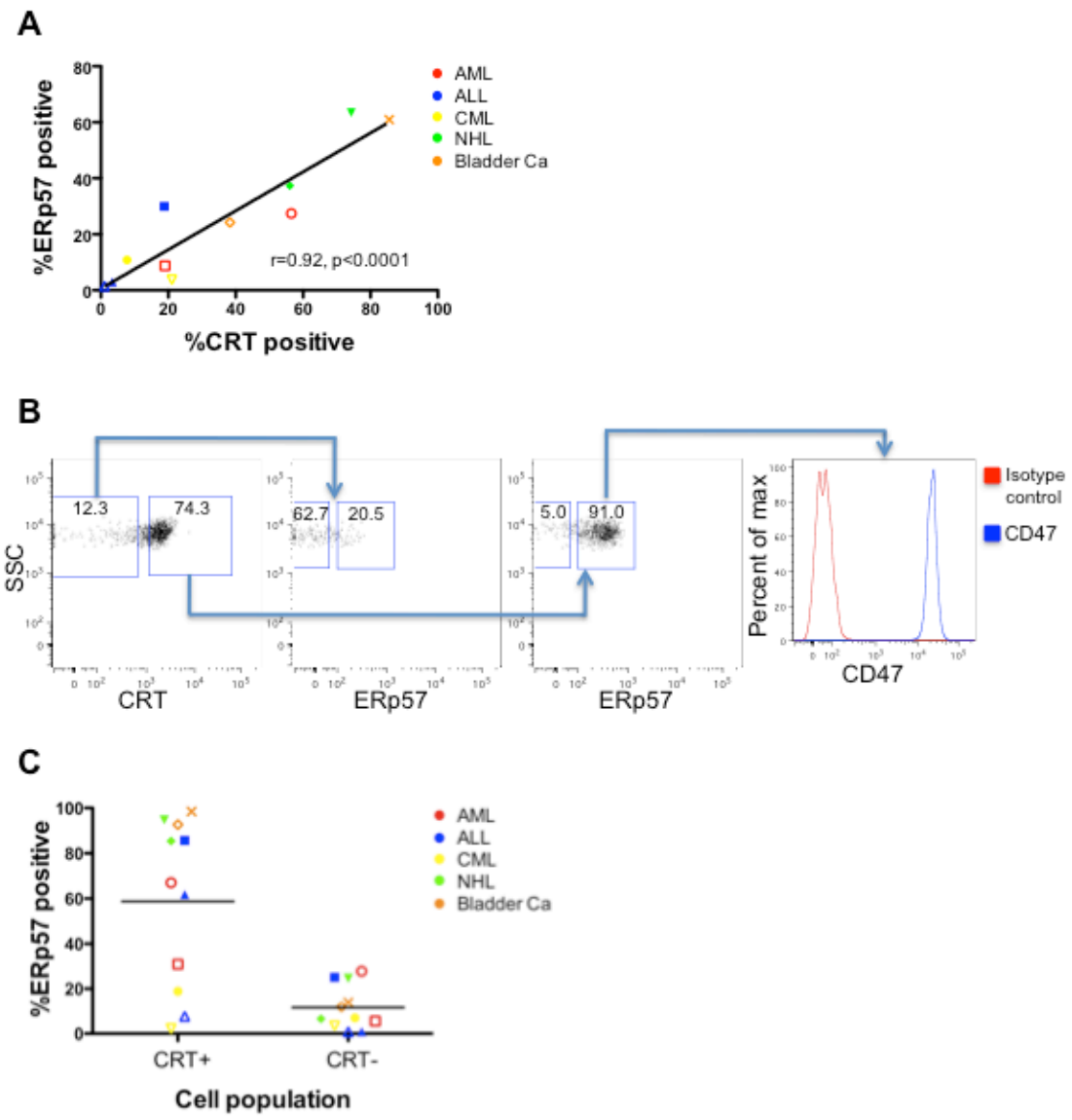

Figure S2: Cell surface CRT correlates with ERp57 expression on tumor cells
(A) A positive correlation between cell surface CRT and ERp57 expression was found on primary human tumors or cancer cell lines using Pearson's correlation coefficient. (B) These cells were analyzed for cell surface expression on ERp57, CRT, and CD47 by flow cytometry. A representative staining profile is shown for Raji cells. A greater percentage of CRT positive cells expressed ERp57 (third panel) compared to CRT negative cells (second panel). CRT+ERp57+ cells also expressed CD47 (fourth panel) in similar levels to the bulk cell population (data not shown). (C) Cell surface ERp57 expression was quantified in CRT+ and CRT- cell populations from several tumor types. A greater percentage of CRT+ cells expressed ERp57 compared to CRT- counterparts (p=0.0006). Each symbol represents a distinct tumor sample. Samples shown were from patient samples or the following cell lines: blue square=Jurkat, green inverted triangle=Raji, green diamond=SUDHL4. All cells profiled in (A-C) were excluded for annexin V-positive cells.

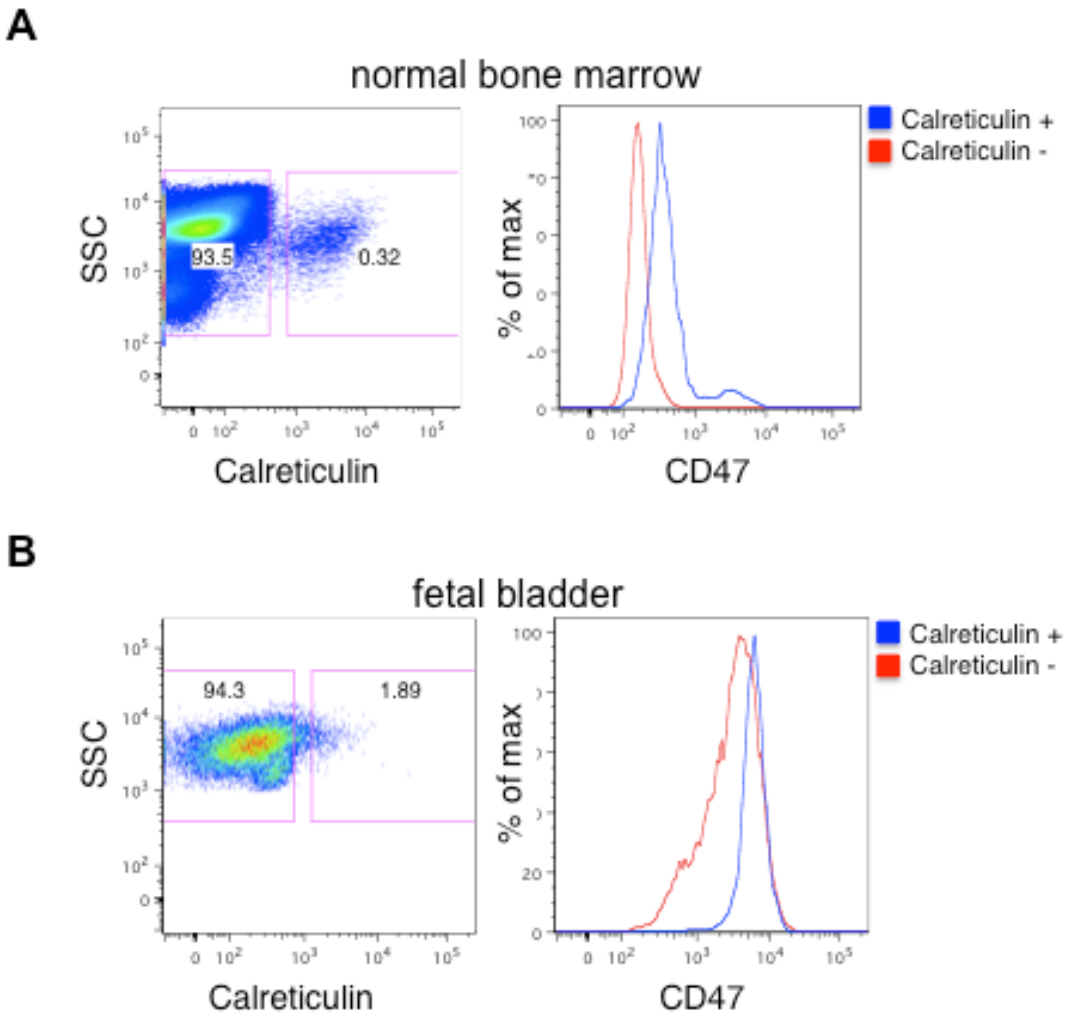

Fig. S3: Live calreticulin positive cells from normal human tissues have higher levels of CD47 compared to calreticulin negative cells

(A,B) Left panel: bulk normal human bone marrow cells (A) or normal human fetal bladder (ESA positive) urothelial cells (B) were profiled for cell surface calreticulin expression by flow cytometry. Right panel: cell surface calreticulin-negative and -positive cells were profiled for CD47 expression, demonstrating higher CD47 expression on calreticulin-positive cells. Annexin V-positive cells were excluded from the analysis of both bulk normal human bone marrow cells and fetal bladder cells. Data is representative of several samples.

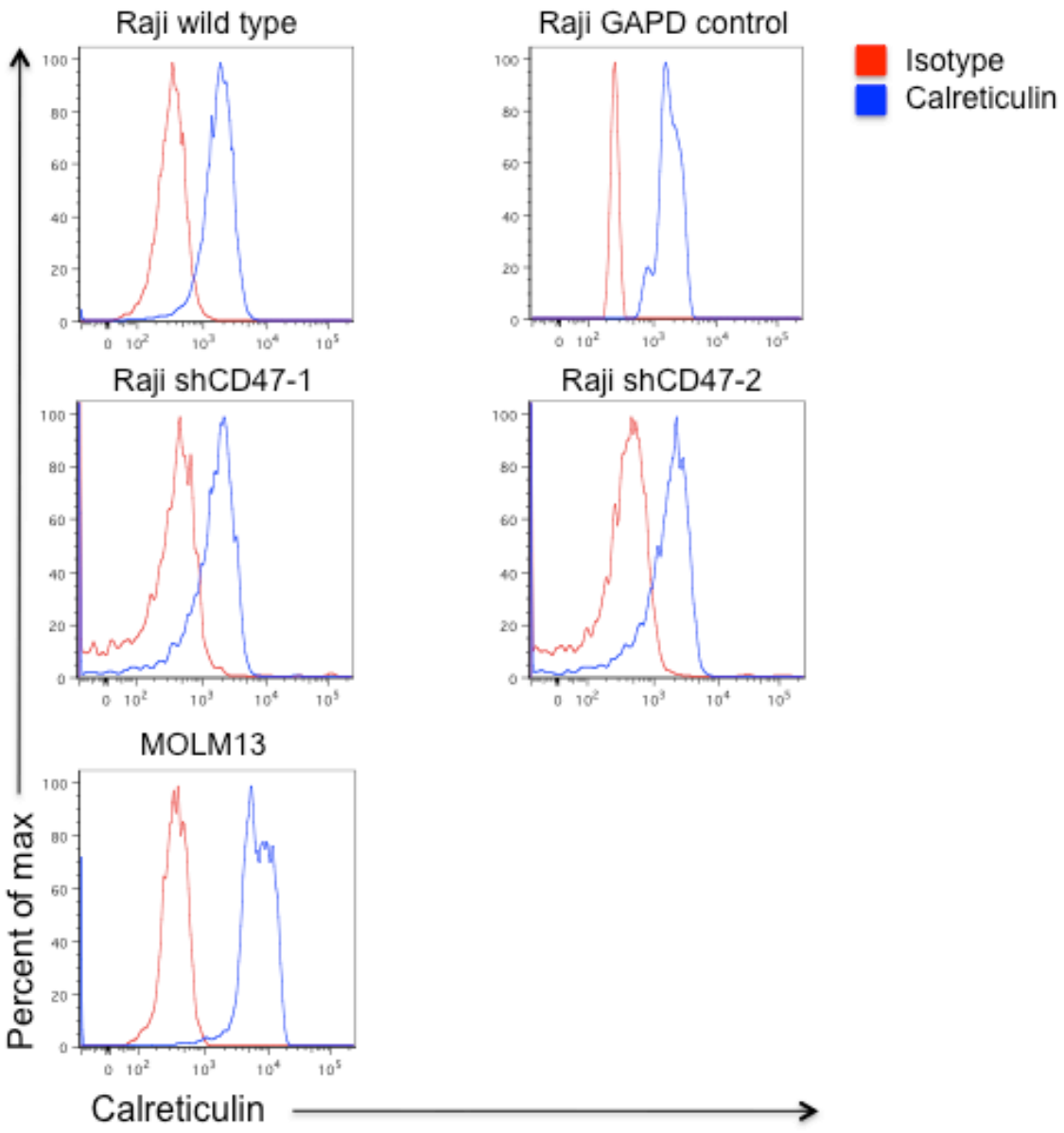

Fig. S4: Calreticulin expression is unaffected by CD47 shRNA knockdown in Raji cells
Raji cells were transduced with lentiviral constructs encoding shRNA directed against CD47 (Raji shCD47-1, shCD47-2) or a GAPD control (Raji GAPD). Cell surface calreticulin expression was determined by flow cytometry and demonstrated no difference on wild type, untransduced Raji cells compared to Raji cells transduced with either GAPD control, shCD47-1, or shCD47-2 lentivirus. Cell surface calreticulin expression for MOLM13 cells is also shown.

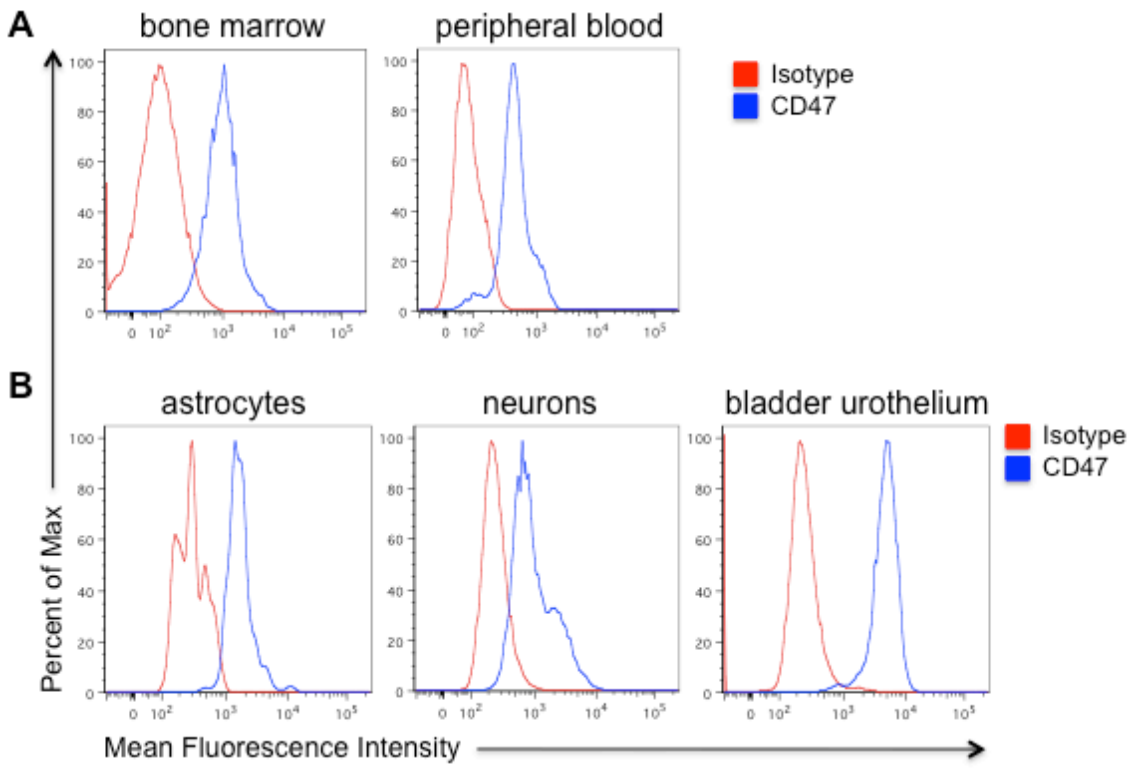

Fig. S5: CD47 is expressed on normal human cells
(A-B) CD47 expression was determined by flow cytometry on normal human hematopoietic cells (A) and fetal tissue cells (B) demonstrating expression on all normal cells profiled. Flow cytometry plots are from a representative sample of each normal tissue cell type.

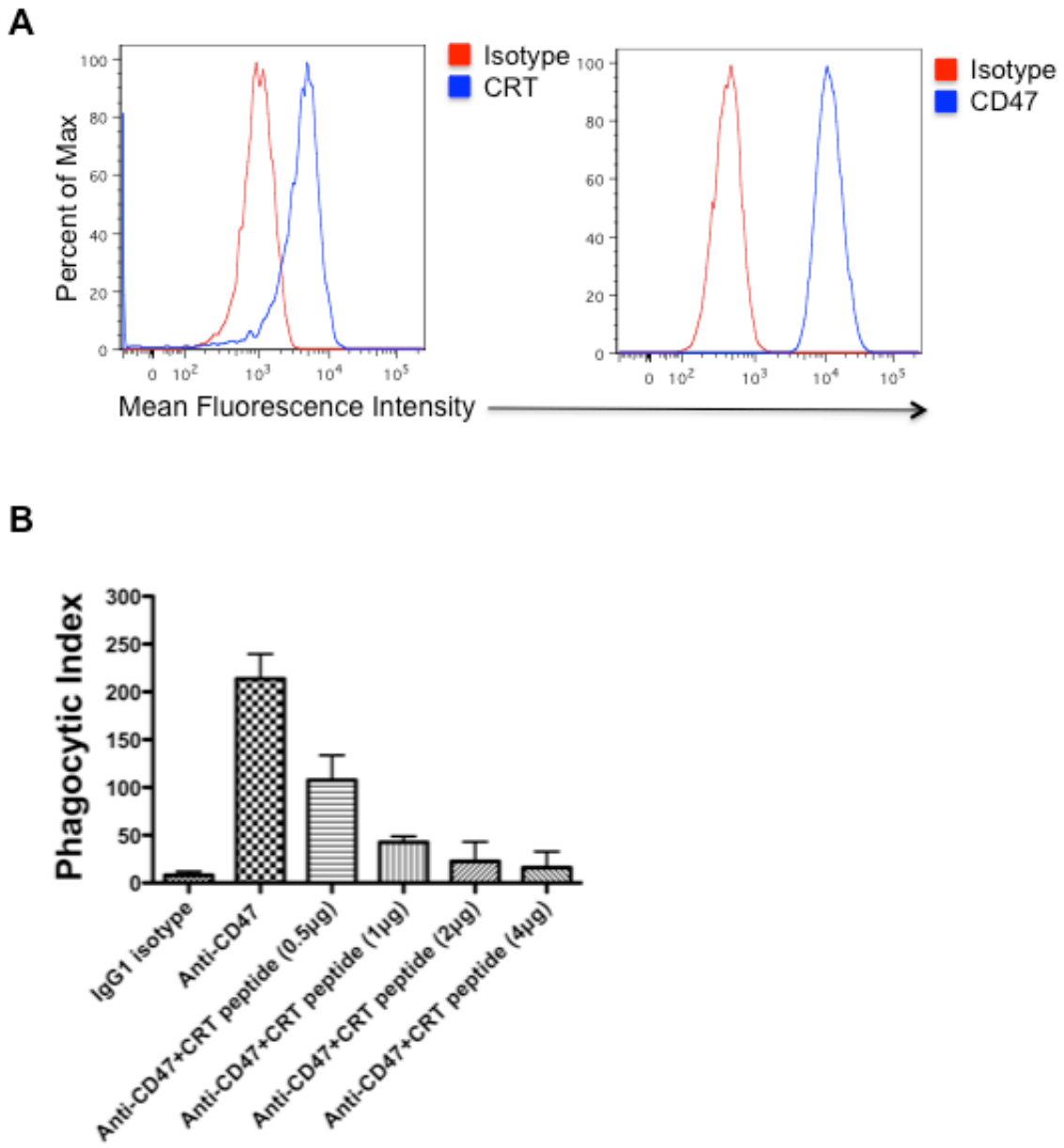

Fig. S6: Abrogation of anti-CD47 antibody-mediated phagocytosis is dose dependent on calreticulin blockade

(A) Cell surface CRT and CD47 expression was determined by flow cytometry on Jurkat cells, a T cell leukemia cell line. (B) Jurkat cells were incubated with human macrophages in the presence of the indicated antibodies and blocking peptides, and phagocytosis was determined by fluorescence microscopy. Anti-CD47 antibody was used at 10µg/ml. CRT blocking peptide concentrations are shown as µg/ml. Each condition was performed in triplicate. Data is expressed as mean ± SD.

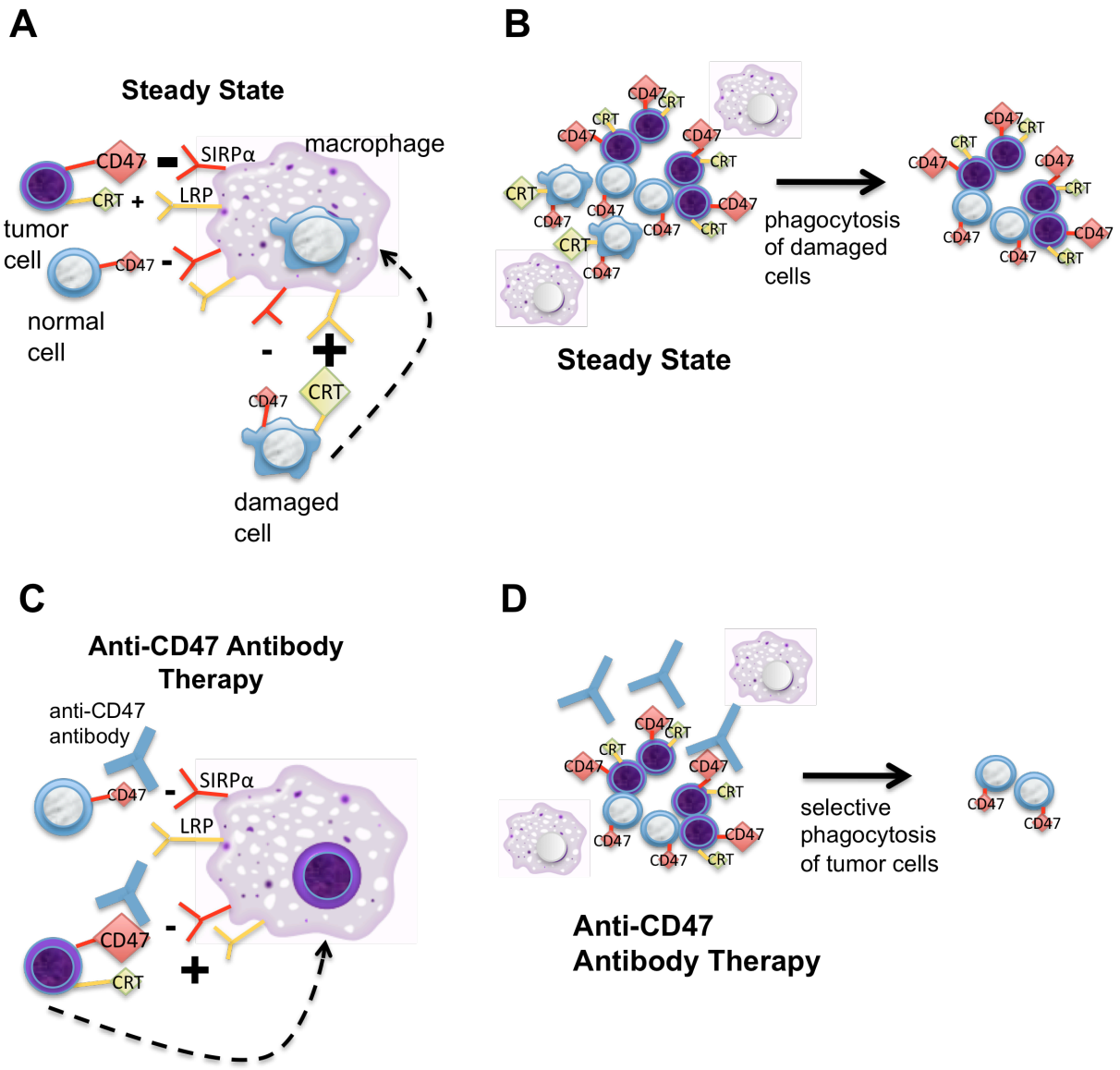

Fig. S7: Model for the integration of pro (CRT)- and anti (CD47)-phagocytic signals on normal and tumor cells at steady state and during anti-CD47 antibody therapy

(A,B) At steady state, tumor, normal, and damaged cells express varying levels of cell surface CD47 and CRT, and it is the integration of both signals that determines whether the target cell will be phagocytosed. Tumor cells express CRT, but also higher levels of CD47 that delivers a dominant negative phagocytic signal (minus sign), leading to evasion of phagocytosis. In contrast, normal cells express lower levels of CD47, but do not express CRT, and thus no phagocytosis occurs. Lastly, damaged or apoptotic cells exhibit high levels of CRT expression, and this positive phagocytic signal (plus sign) dominates over low CD47 expression, leading to phagocytosis (dashed arrow). (C,D) During anti-CD47 antibody therapy, the negative phagocytic stimulus (CD47) is blocked. In tumor cells, this unmasks the positive phagocytic signal (CRT), leading to phagocytosis. In contrast, normal cells are not phagocytosed since the positive phagocytic stimulus (CRT) is absent.

Disease (dataset)	Fig.	Data source	Patients (n)	Therapy	Dichotomous (median)			Continuous			Ref
					HR	95% CI	P value	HR	Z-score	P value	
Neuroblastoma (1)	4A	EBI Array Express: E-MTAB-179	478	obs, surgery, L to HR-CX^{+}	1.70	1.23-2.35	<0.005	2.25	4.07	<0.0001	50
Neuroblastoma (2)	4B	EBI Array Express: E-TABM-38	251	Obs, surgery, CTX, VCR, cisplatin, DOX	1.78	1.10-2.87	<0.05	4.78	3.11	<0.005	51
Superficial and invasive bladder cancer (1)	4C	NCBI GEO: GSE13507	165*	BCG, radical cystectomy /LN dissection, cisplatin-based chemo	2.52	1.17-5.45	<0.05	3.36	3.48	<0.001	52
Invasive bladder cancer (2)	4D	NCBI GEO: GSE5287	30	cisplatin-based chemo	2.18	0.95-4.98	0.059	2.53	1.99	<0.05	53
Mantle cell lymphoma (1)	4E	NCBI GEO: GSE10793	71	untreated	2.57	1.35-4.89	<0.005	3.02	3.19	<0.005	54
Mantle cell lymphoma (2)	4F	LLMPP: Rosenwald MCL	92	multi-agent chemo	3.06	1.72-5.43	<0.0001	1.72	4.12	<0.0001	55

Table S1: Analysis of the prognostic value of calreticulin expression in human malignancies
Summary of statistical analyses is presented from clinical data in figure 4. Dichotomous HR and associated statistics reflect *calreticulin* expression cut-off around the median. Statistics are also presented for *calreticulin* expression when considered as a continuous variable with log-likelihood p values within a univariate Cox regression model. Therapy represents all possible therapies administered within each cohort. $^{+}$first line therapy. *91 patients in this dataset had missing clinical data. Ref=reference, HR=hazard ratio, CI=confidence interval, obs=observation, L to HR-CX=low (<2 cycles) to high dose (≥6 cycles) cytotoxic therapy, BCG=bacillus calmette-guerin immunotherapy, CTX=cyclophosphamide, VCR=vincristine, DOX=doxorubicin, LN=lymph node.